

THERMAL MODELLING OF LINE START PERMANENT MAGNET SYNCHRONOUS MOTOR

This thesis is submitted to fulfil the requirement of the degree

Master in Electrical Engineering

Submitted by
SANDIPAN DUTTA

Examination Roll no. – **M4ELE23018**
Registration no. – **160171 of 2021-2022**

Under the guidance of
PROF. SUPARNA KAR CHOWDHURY
PROF. ARINDAM KUMAR SIL
PROF. DIPTEN MAITI

Department of Electrical Engineering
Jadavpur University
Kolkata – 700032

Certificate

This is to certify that the thesis entitled “Thermal Modelling of Line Start Permanent Magnet Synchronous Motor”, submitted by Mr. Sandipan Dutta (Examination Roll No. M4ELE23018), under our supervision and guidance during the session of 2021-23 in the department of Electrical Engineering, Jadavpur University. We are satisfied with his work, which is being presented for the partial fulfilment of the degree of Master in Electrical Engineering from Jadavpur University, Kolkata-700032.

Prof. Suparna Kar Chowdhury
Professor
Department of Electrical
Engineering
Jadavpur University
Kolkata, 700032

Prof. Arindam Kumar Sil
Associate Professor
Department of Electrical
Engineering
Jadavpur University
Kolkata, 700032

Prof. Dipten Maiti
Assistant Professor
Department of Electrical
Engineering
Jadavpur University
Kolkata, 700032

Prof. Biswanath Roy
Head of the Department of
Electrical Engineering
Jadavpur University
Kolkata, 700032

Prof. Saswati Mazumdar
Dean of Faculty Council of
Engineering and Technology
Jadavpur University
Kolkata, 700032

Faculty of Engineering and Technology Jadavpur
University, Kolkata - 700 032

Certificate of Approval

The forgoing thesis entitled “**Thermal Modelling of Line Start Permanent Magnet Synchronous Motor**” is hereby approved as a creditable study of an Engineering subject carried out and presented in a manner that fulfils its acceptance as a prerequisite to the degree for which it is submitted. It is understood that by this approval, the undersigned does not necessarily endorse or approve any statement made, opinion expressed, or conclusion drawn therein but approves the thesis only for the purpose for which it is submitted.

The final examination for evaluation of the thesis

Signature of the examiners

.....

.....

.....

.....

Declaration of Originality

I hereby declare that this thesis contains a literature survey and original research work done by me. All the information in this document has been obtained and presented according to academic rules and ethical conduct. I also declare that, as required by these rules and conduct, I have fully cited and referenced all material and results that are not original to this work.

Name: Sandipan Dutta

Examination Roll No: **M4ELE23018**

University Registration No: **160171 of 2021-2022**

Thesis Title: **Thermal Modelling of Line Start Permanent Magnet Synchronous Motor**

Signature with Date:

ACKNOWLEDGMENTS

I express my sincere gratitude to my supervisor, Prof. Suparna Kar Chowdhury for her encouragement, suggestion, and advice, without which it would not have been possible to complete my thesis successfully. I would like to thank Prof. Arindam Kumar Sil and Prof. Dipten Maiti for being a constant source of encouragement, inspiration and for their valuable suggestions coupled with their technical expertise throughout my research work. It was a great honor for me to pursue my research under their supervision.

I would also extend my gratitude to my co-worker, Mrs. Mousumi Jana Bala, a research scholar within our department. Her unwavering support and continuous encouragement during the course of my thesis work have been invaluable. Additionally, I would like to express my appreciation to all the members of the Drives and Simulation laboratory for their various forms of assistance throughout this journey.

I would also like to express my sincere gratitude to Mr. Sowmitro Jana, Director of Vikrant Special Machines Pvt. Ltd., for his unwavering support and for providing me with the opportunity to achieve this milestone. Without his involvement, this achievement would never have been possible. I am truly grateful for the opportunity he gave me and for his belief in me, which enabled me to transform my dream into a reality.

Finally, I extend my words of gratitude to my family for personally motivating me to carry out the work smoothly.

I also extend my heartfelt gratitude to the Almighty for the wisdom, strength, and inspiration provided me during this course of journey.

ABSTRACT

A thermal model of the Line Start Permanent Magnet Synchronous Motor (LSPMSM) has been developed in this thesis to predict the motor's temperature rise under operating condition. The model utilizes the lumped parameter method and accounts for the heat generation within the motor.

Simulation has been performed using MATLAB software. The thermal model can be used to optimize the design and operation of LSPMSMs. It can be used to predict the motor's temperature rise under different operating conditions and to identify the factors that contribute to overheating. This information can be used to design motors that are more resistant to overheating and to operate motors in a way that minimizes their temperature rise. The thesis also discusses about the scope for future research.

TABLE OF CONTENT

CHAPTER NO.	CONTENTS	PAGE NOS.
	Acknowledgement	4
	Abstract	5
	Table of content	6-7
	List of Acronyms	8
	List of symbols used	9-10
	List of figures	11
	List of tables	12
1	Introduction	13-14
1.1	Motivation of Work	14-15
1.2	Literature Review	15-18
1.3	Organization of Thesis	18
2	Construction of Synchronous motors	19-20
2.1	Rotor configurations	22
2.1.1	Merrill's rotor	22-23
2.1.2	Interior-type PM motors	23
2.1.3	Surface PM motors	23
2.1.4	Inset-type PM rotor	23-24
2.1.5	Buried PM motors	24
3	The Line-Start Permanent Magnet Synchronous Motor	26
3.1	Equivalent circuit model	27
3.2	Mathematical model of LSPMSM	28-30
4	Thermal Modelling Background	31
4.1	Heat Transfer Mechanisms	32-33
4.1.1	Thermal Resistance of Solids	33
4.1.2	Thermal Resistance of Gases and Fluids	34-35
4.2	Thermal Resistance Network Modelling	35-36
4.3	Thermal Network Modelling Method	36
4.3.1	Nodalization	36-37
4.3.2	Lumped Parameter Thermal Element	37-38
4.4	Development of thermal network	38
4.4.1	Calculation of Resistance between Frame and Ambient	38

4.4.2	Calculation of Frame Contact Resistance	39
4.4.3	Calculation of Thermal Resistance of Air gap	39-40
4.4.4	Calculation of Thermal Resistance with End Shield	40-41
4.4.5	Plane Wall with Specified Boundary Temperatures	41
4.4.6	Cylinders with Specified Temperature	41
4.4.7	Calculation of Thermal Capacitances	42
5	A Lumped Parameter Thermal Network Model (LPTN)	43
5.1	LPTN model and simulation	44-45
5.2	Results and observation	47-50
6	Conclusions	51-52
6.1	Future scope of work	52
	References	53-56

LIST OF ACRONYMS

ABBREVIATIONS

IM

INDUCTION MOTOR

LSPMSM

LINE START PERMANENT
MAGNET SYNCHRONOUS
MOTOR.

PMSM

PERMANENT MAGNET
SYNCHRONOUS MOTOR.

TEFC

TOTALLY ENCLOSED, FAN-
COOLED

PM

PERMANENT MAGNET

AC

ALTERNATING CURRENT

DC

DIRECT CURRENT

RPM

REVOLUTIONS PER MINUTE

SPM

SURFACE MOUNTED
PERMANENT MAGNET
INTERIOR PERMANENT
MAGNET

IPM

SIPM

SURFACE INSET
PERMANENT MAGNET
COMPUTATIONAL FLUID
DYNAMICS

CFD

FEM

FEM

LPTN

LUMPED PARAMETER
THERMAL NETWORK

LIST OF SYMBOLS

SYMBOL	MEANING
h_M	height of the permanent magnet
α_i	effective pole arc coefficient $\alpha_i = b_p/\tau$
E_f	Induced EMF
T_{em}	electromechanical torque
T_{cg}	cage torque
T_{pm}	permanent magnets torque
r_s	per-phase stator winding resistance
$L_{\sigma s}$	per-phase stator leakage inductance
r'_r	per-phase rotor circuit resistance
$L_{\sigma' r}$	per-phase rotor leakage inductance
E_f	back-EMF
L_m	per-phase stator magnetizing inductance
ω	is the angular speed
r_s	rotor resistance
V_{qd0s}, V_{qd0r}	are the q, d, 0 axis of the stator and rotor voltages
i_{qd0s}, i_{qd0r}	are the q, d, 0 axis of the stator and rotor currents
$\lambda_{qd0s}, \lambda_{qd0r}$	are the q, d, 0 axis of the stator and rotor flux linkages
r_b	is the rotor bar resistance
N_s	is the number of stator winding turns
L_{ls}	is the stator leakage. L'_{lr} is the rotor leakage
$L_{mq,d}$	is the q, d axis of the magnetizing inductances
J	is the rotor moment of inertia
ω_m	is the angular speed
P	is the number of poles
T_e and T_L	are the electromagnetic and load torques
λ	is the thermal conductivity
L	is the distance between the nodes
α	is the heat transfer coefficient
Nu	Nusselt number
\emptyset	Angle, temperature
G	Thermal conductance matrix

θ	Temperature vector
h	boundary film coefficient
A_c	surface area in contact with the cooling air.
Q	Rate of heat flow
K	Thermal conductivity
δ_x	Thickness of the plate.
T_1, T_2	Temperatures of the two faces of the wall
K_x	thermal conductivity along X direction
K_y	thermal conductivity along Y direction
Q^*	internal generated heat per unit volume
ρ	the density of the material
C_p	the specific heat of the material
C_{th}	Thermal capacity
V_n	volume of the segment
ρ_v	density of the material
C_{ths}	specific heat

LIST OF FIGURES

Figure No.	Figures	Page No.
Fig – 2 : (a)	Classical configuration of rotor	20
Fig – 2: (b)	Interior-magnet rotor	21
Fig – 2: (c)	Surface-magnet rotor	21
Fig – 2: (d)	Inset-magnet rotor	21
Fig – 2: (e)	Rotor with buried (spoke) magnets symmetrically distributed	22
Fig – 2:(f)	Rotor with buried magnets asymmetrically distributed	22
Fig. 2.1.5 (a)	improperly designed rotor with ferromagnetic shaft	25
Fig. 2.1.5 (b)	rotor with non-ferromagnetic shaft	25
Fig. 3 (a)	Cross section of a three phase LS PMSM	26
Fig. 3 (b)	Boot profile of a LS PMSM	27
Fig. 3 (c)	Per phase equivalent circuit model of a LS PMSM	28
Fig.5 (a)	Schematic diagram of LPTN model	46
Fig.5 (b)	Simulated temperature rise in frame of Motor	47
Fig.5 (c)	Simulated temperature rise in stator core of Motor	47
Fig.5 (d)	Simulated temperature rise in stator conductor of Motor	48
Fig.5 (e)	Simulated temperature rise in rotor upper core of Motor	48
Fig.5 (f)	Simulated temperature rise in PM of Motor	49
Fig.5 (g)	Simulated temperature rise in rotor lower core of Motor	49

LIST OF TABLES

Table No.	Table	Page No.
1	Rotor configurations for PM synchronous motors	20-22
2	The relation between some electric and thermal quantities	31
3	Motor name plate data	44

Chapter 1

Introduction

In contemporary times, small three-phase induction motors (IMs) find extensive use across various industrial sectors, including applications like pumps and fans. Despite their cost-effectiveness, these small IMs typically exhibit relatively low operational efficiency and power factor. Given the growing concern for environmental issues and global warming, there's a heightened interest in enhancing the energy efficiency of the numerous IMs currently in use in industry. The introduction of legislation further amplifies the demand for more efficient motors.

While small permanent magnet synchronous machines can achieve remarkable operational efficiency and power factor, they lack the starting capability possessed by induction motors (IMs). To bridge this gap, the line-start permanent magnet synchronous motor (LSPMSM) has been developed. The LSPMSM utilizes a rotor cage to generate the initial starting torque required to synchronize the motor, while it relies on permanent magnets for producing synchronous torque during steady-state operation. Because it operates in essence as a synchronous motor, the induced current and resulting copper losses in the rotor cage are minimal. Additionally, the motor maintains a high power factor, similar to conventional permanent magnet synchronous motors, which further reduces stator current and associated losses.

Past research on LSPMSMs has primarily focused on higher-power applications, where large-scale IMs have served as a benchmark for machine design. While achieving high efficiency and good power factor in larger LSPMSMs can be relatively straightforward through parameter

optimization, they encounter significant challenges due to the complex manufacture and assembly of large permanent magnets.

In contrast, smaller IMs experience reduced efficiency and power factor due to a higher penalty factor associated with field excitation. Therefore, there has been considerable interest in incorporating permanent magnets into the rotor core of small IMs to mitigate the excitation penalty and consequently enhance efficiency. Unlike their larger counterparts, it has been relatively simpler to integrate small permanent magnets into the rotor core of small IMs. This suggests that optimized LSPMSMs could potentially be developed by skillfully modifying existing small IMs, thereby saving significant resources that would otherwise be spent on redesigning and replacing motors to achieve higher operational efficiency.

1.1 Motivation of work

Permanent magnet synchronous motors (PMSMs) are gaining increasing popularity across various applications due to their exceptional efficiency and performance attributes. However, the elevated temperatures generated during PMSM operation can trigger thermal challenges, including magnet demagnetization and a shortened motor lifespan.

Thermal modeling stands as a valuable tool for comprehending and forecasting the thermal behavior of PMSMs. By precisely simulating heat transfer processes and thermal resistances within the motor, it becomes feasible to pinpoint critical components and engineer for optimal thermal efficiency.

This thesis concentrates on the thermal modeling of a specific PMSM subtype, known as line-start PMSMs. These PMSMs possess the unique ability to initiate operation directly from the mains, eliminating the need for an external starter. While this feature makes them a convenient and

cost-effective choice for certain applications, line-start PMSMs are also more susceptible to thermal challenges compared to other PMSM types.

The primary objective of this thesis is to establish a comprehensive thermal model for a line-start PMSM for prediction of its thermal performance.

The model serves as a crucial tool for identifying critical components and optimizing the design to enhance thermal efficiency.

1.2 Literature review

The hybrid lumped-parameter and two-dimensional analytical thermal model for electrical machines are presented in paper [1], combining the accuracy of two-dimensional thermal models with the computational efficiency of lumped-parameter models. Validation against experimental data for a permanent magnet synchronous motor (PMSM) demonstrates that the temperature distribution in the PMSM can be accurately predicted by the proposed model.

A simple lumped-parameter thermal model [2] has been presented for an electrical machine with a totally enclosed fan-cooled (TEFC) design, considering heat dissipation from the stator windings, rotor core, and rotor windings. Experimental data validation for a three-phase induction motor shows that the temperature rise in the motor can be accurately predicted by the proposed model.

The paper [3] deals with the thermal modelling of PMSM using Lumped Parameter Thermal Network (LPTN) and FE (Finite Element) model. Lumped-parameter thermal model has been presented, taking into account heat dissipation from the stator windings, rotor core, rotor magnets, and bearings. Experimental data validation for a PMSM demonstrates that the

temperature rise in the PMSM can be accurately predicted by the proposed model.

In this paper [4] an analytical thermal model for a PMSM demonstrates the heat dissipation from the stator windings, rotor core, and rotor magnets. Development and analysis of a new generic steady state thermal model for mapping the heat transfer throughout a permanent magnet synchronous motor by considering its individual components as elements of an overall thermal equivalent circuit. Experimental data validation for a PMSM shows that the temperature rise in the PMSM can be accurately predicted by the proposed model.

The paper [5] presents hybrid thermal model for electrical machines. Combined lumped-parameter and two-dimensional models, has been proposed and validated for the prediction of temperature distribution in IPMSM. The 2-D analytical thermal models are obtained by solving the Poisson's equations with the Dirichlet boundary conditions extracted from the LPTN.

C. Liu presented and validated a thermal computation model for PMSMs in this paper [6], for accurate temperature distribution prediction. The model has been useful for motor design and cooling system optimization.

An Electromagnetic and Thermal Comparison Study has been presented in this paper [8]. Inner and outer rotor line-start PMSMs are compared in the paper with inner rotors found to offer higher torque and efficiency, albeit with a greater temperature rise.

The impact of temperature on permanent magnet demagnetization in LSPMSMs has been investigated in this paper, showing significant increases during start up, depending on motor design and conditions.

The paper [13] presents performance analysis of LSPMSM for Electric Vehicles for different rotor configuration, in terms of torque, efficiency, and starting current. The results show that the IPM rotor has the best performance in terms of all three metrics. The salient-pole rotor has the worst performance, while the conventional rotor has an intermediate performance.

In paper [14] impact of temperature on partial demagnetization in a line start permanent magnet synchronous motor (LSPMSM) has been explored. A 2D field-circuit model has been employed to simulate both electromagnetic and thermal motor behaviour. Findings indicate that temperature rises significantly during start up, potentially causing partial demagnetization. The extent of demagnetization has been shown to vary based on motor design and operating condition.

In paper [20] a real-time thermal model of a permanent-magnet synchronous motor (PMSM) based on the geometry of the different components of the motor has been developed. The model has been implemented in a digital signal processor (DSP) and has been shown to be accurate in all operating conditions, including steady-state, transient, and stall torque.

The paper [22] deals with the development of a simple and accurate formulation for calculating convective heat transfer in electric machines. This formulation can be used to improve the accuracy of thermal models of electric machines, which is important for thermal management and fault diagnosis.

These are some of the many papers that have been published on thermal modelling of electrical machines. The choice of a particular thermal model will depend on the specific application.

1.3 Organization of Thesis

Chapter 1: Outlines the preliminary concept of thesis work. It contains a brief history of PMSM, my motivation for this work and an outlook about the different chapters and topic of discussion in this thesis.

Chapter 2: Chapter 2 deals with construction of Synchronous motors with different rotor configurations.

Chapter 3: Chapter 2 deals with general overview, construction, equivalent circuit and mathematical model of LSPMSM.

Chapter 4: Chapter 4 deals with background of thermal modelling, heat transfer mechanism, thermal resistance network modelling and calculation of thermal resistances, capacitances.

Chapter 5: Chapter 5 is all about Modelling of Lumped Parameter Thermal Network model in Matlab software environment and simulating temperature rise in different machine parts.

Chapter 6: Chapter 6 outlines some conclusion and different avenues for future work.

Chapter 2

Construction of Synchronous motors

Synchronous motors maintain a consistent rotational speed that perfectly aligns with the frequency of the power source. These motors are categorized based on their rotor's design, construction, materials, and operational characteristics, forming the fundamental four groups [16]:

- Electromagnetically-excited motors
- PM motors
- Reluctance motors
- Hysteresis motors

In electromagnetically excited and PM motors a cage winding is frequently mounted on salient-pole rotors to provide asynchronous starting and to damp oscillations under transient conditions, so-called damper. Recent developments in rare-earth PM materials and power electronics have opened new prospects on the design, construction and application of PM synchronous motors. Servo drives with PM motors fed from static inverters are finding applications on an increasing scale. PM servo motors with continuous output power of up to 15 kW at 1500 rpm are common. Commercially, PM A.C. motor drives are available with ratings up to at least 746 kW. Rare-earth PMs have also been recently used in large power synchronous motors rated at more than 1 MW. Large PM motors can be used both in low-speed drives (ship propulsion) and high-speed drives (pumps and compressors).

PM synchronous motors are usually built with one of the following rotor configurations:

- (a) Classical (F. Merrill's rotor, US patent 2543639 assigned to General Electric), with salient poles, laminated pole shoes and a cage winding (Fig. 2a);
- (b) interior-magnet rotor (Fig. 2b);
- (c) surface-magnet rotor (Fig. 2c);
- (d) inset-magnet rotor (Fig. 2d);
- (e) Rotor with buried magnets symmetrically distributed (Fig. 2e);
- (f) Rotor with buried magnets asymmetrically distributed according to German patent 1173178 assigned to Siemens, also called Siemosyn (Fig. 2f).

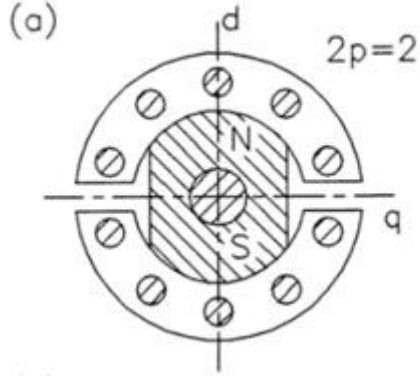
Table - 1 - Rotor configurations for PM synchronous motors	
<p>Fig – 2 : (a) Classical configuration (US patent 2543639)</p>	

Fig – 2: (b) Interior-magnet rotor

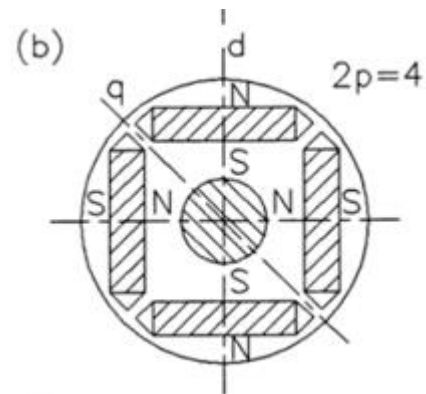


Fig – 2: (c) Surface-magnet rotor

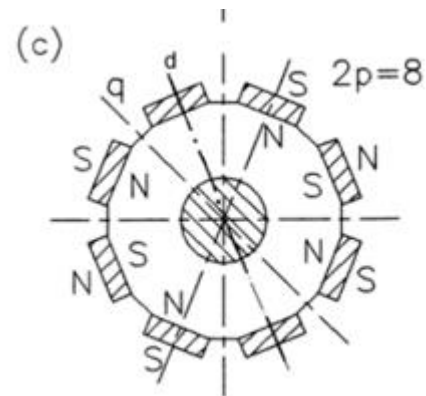
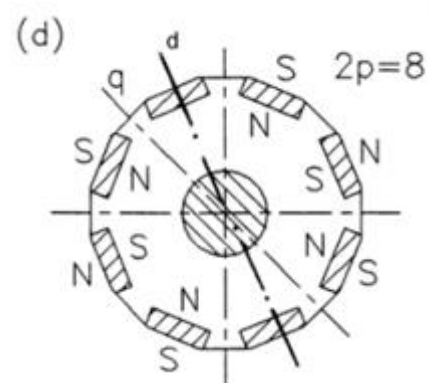
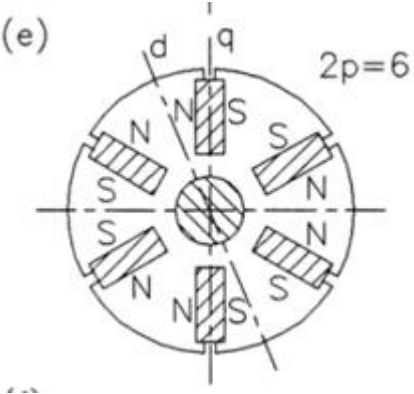
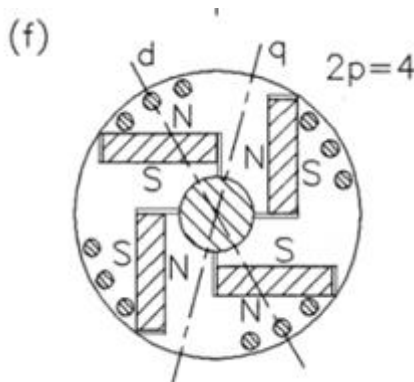


Fig – 2: (d) Inset-magnet rotor



<p>Fig – 2: (e) Rotor with buried (spoke) magnets symmetrically distributed</p>	
<p>Fig – 2:(f) Rotor with buried magnets asymmetrically distributed (German patent 1173178)</p>	

2.1 Rotor configurations

2.1.1 Merrill's rotor

The first successful construction of a PM rotor for small synchronous motors rated at high frequencies was patented by F.W. Merrill (US patent 2543639). It was a four-pole motor similar to the two-pole motor shown in Fig. 2a. The laminated external ring has deep narrow slots between each of the PM poles (Fig. 2a). Owing to cage rotor winding the motor is self-starting.

The leakage flux produced by the PM can be adjusted by changing the width of the narrow slots. The Alnico PM is protected against demagnetization because the armature flux at starting and reversal goes

through the laminated rings and narrow slots omitting the PM. The PM is mounted on the shaft with the aid of an aluminum or zinc alloy sleeve. The thickness of the laminated rotor ring is chosen such that its magnetic flux density is approximately 1.5 T when the rotor and stator are assembled. Magnetic flux density in the rotor teeth can be up to 2 T.

2.1.2 Interior-type PM motors

The interior-magnet rotor has radially magnetized and alternately poled magnets (Fig. 2b). Because the magnet pole area is smaller than the pole area at the rotor surface, the air gap flux density on open circuit is less than the flux density in the magnet. The synchronous reactance in d-axis is smaller than that in q-axis since the q-axis magnetic flux can pass through the steel pole pieces without crossing the PMs. The magnet is very well protected against centrifugal forces. Such a design is recommended for high frequency high speed motors.

2.1.3 Surface PM motors

The surface magnet motor can have magnets magnetized radially (Fig. 2c) or sometimes circumferentially. An external high conductivity non-ferromagnetic cylinder is sometimes used. It protects the PMs against the demagnetizing action of armature reaction and centrifugal forces, provides an asynchronous starting torque, and acts as a damper. If rare-earth PMs are used, the synchronous reactance's in the d- and q-axis are practically the same.

2.1.4 Inset-type PM rotor

In the inset-type motors (Fig. 2d) PMs are magnetized radially and embedded in shallow slots. The rotor magnetic circuit can be laminated or made of solid steel. In the first case a starting cage winding or external non-ferromagnetic cylinder is required. The q-axis synchronous reactance is

greater than that in the d-axis. In general, the EMF E_f induced by the PMs is lower than that in surface PM rotors.

2.1.5 Buried PM motors

The buried-magnet rotor has circumferentially magnetized PMs embedded in deep slots (Fig. 2e). Because of circumferential magnetization, the height h_M of the PM is in tangential direction, i.e., along the pole pitch. The effective pole arc coefficient α_i is dependent on the slot width. The synchronous reactance in q-axis is greater than that in d-axis. A starting asynchronous torque is produced with the aid of both a cage winding incorporated in slots in the rotor pole shoes (laminated core) or solid salient pole shoes made of mild steel. The width of the iron bridge between the inner ends of the neighbouring magnets has to be carefully chosen. The application of a non-ferromagnetic shaft is essential (Fig. 2.1.5). With a ferromagnetic shaft, a large portion of useless magnetic flux goes through the shaft (Fig. 2.1.5a). A buried-magnet rotor should be equipped with a non-ferromagnetic shaft (Fig. 2.1.5b) or a non-ferromagnetic sleeve between the ferromagnetic shaft and rotor core should be used.

Magnetic flux distribution in the cross section of a buried-magnet synchronous motor:

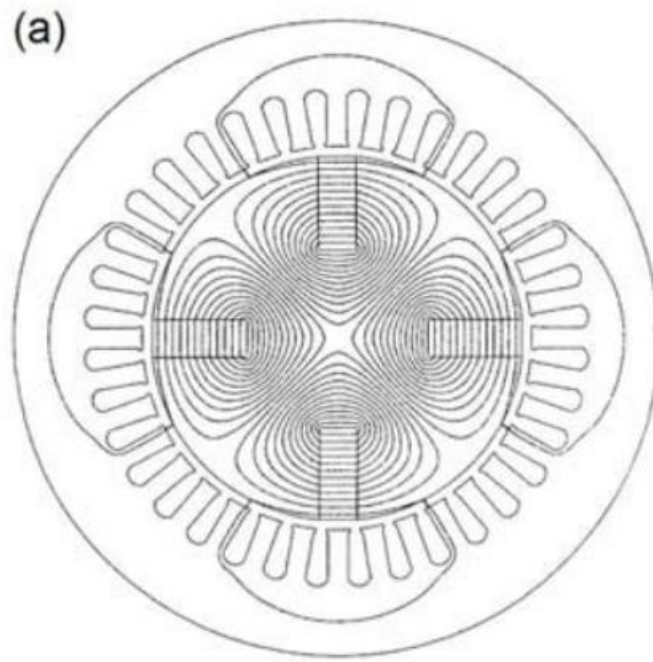
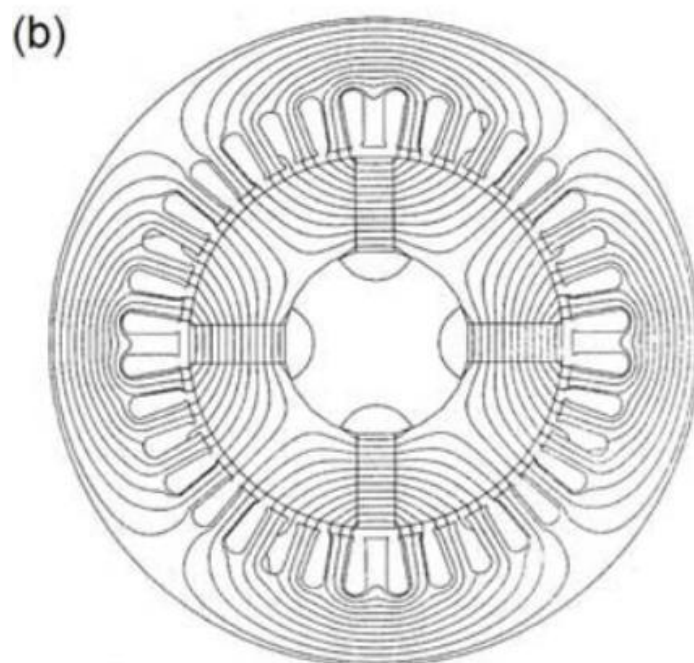


Fig. 2.1.5 (a) Improperly designed rotor with ferromagnetic shaft, (b) Rotor with non-ferromagnetic shaft.



Chapter 3

The Line-Start Permanent Magnet Synchronous Motor (LSPMSM).

A LSPMSM is a combination of a permanent magnet synchronous motor (PMSM) and of an induction motor (IM). [9] The rotor is formed by permanent magnets and a squirrel cage, as seen in Figure 3.

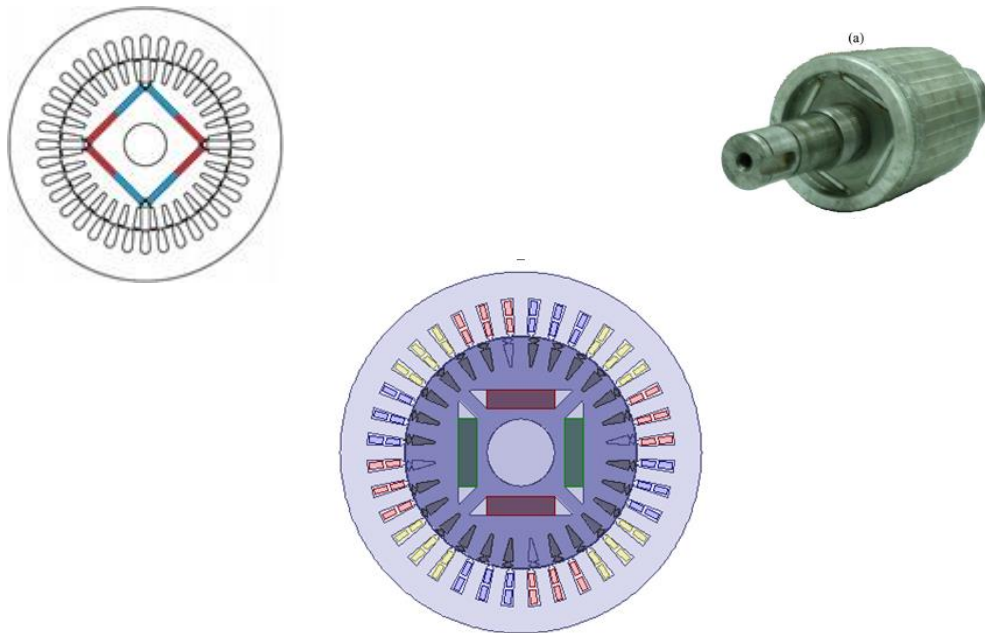


Figure 3 (a) – Cross section of a three phase LS PMSM

For a cylindrical poles motor, during the transient period, the electromechanical torque (T_{em}) is given by the combined contribution of both cage torque (T_{cg}) and permanent magnets torque (T_{pm}). In this period, T_{pm} present an oscillatory nature, as can be seen in Figure 3b. During the steady state regime, at synchronous speed, the electromechanical torque is only given by the permanent magnets because no currents are induced in the rotor. Thus, total losses and general temperature are minimized, increasing the LS PMSM efficiency potential when compared with IM.

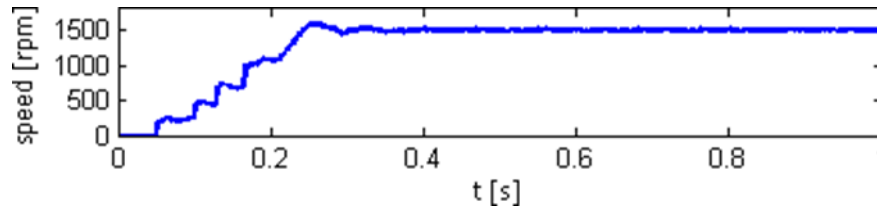


Figure 3 (b) – Boot profile of a LS PMSM.

3.1 Equivalent circuit model

Based on the equivalent circuit of the induction machine (IM) recommended by IEEE, and the conventional permanent magnet synchronous motor (PMSM) equivalent circuit, line-started permanent magnet synchronous motors (LS PMSM) are represented by a hybrid, per phase, equivalent circuit model presented in Figure 3 (c), where:

- r_s – per-phase stator winding resistance;
- $L\sigma_s$ – per-phase stator leakage inductance;
- r'_r – per-phase rotor circuit resistance;
- $L\sigma'_r$ – per-phase rotor leakage inductance;
- E_f – back-EMF;
- L_m – per-phase stator magnetizing inductance.

It is possible to notice in Figure 3(c) some technical features of the squirrel cage ($L\sigma'_r$ and r'_r) and of the rotor magnets (E_f).

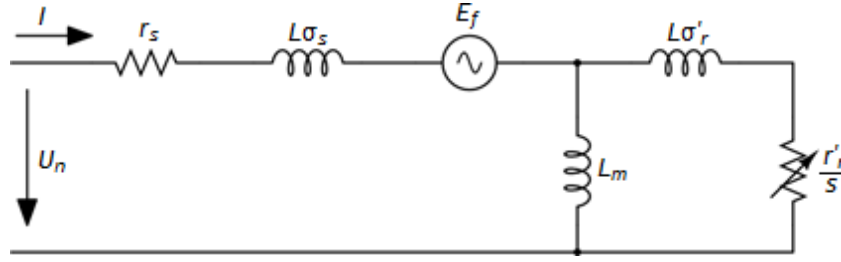


Figure 3 (c) – Per phase equivalent circuit model of a LS PMSM.

3.2 Mathematical model of LSPMSM

The line start permanent magnet synchronous motor has the characteristics of high efficiency synchronous motors with self-starting capability when connected to a fixed frequency voltage source. Synchronous excitation provided to the motor when the permanent magnets installed on its rotor. In addition, cage torque provides the motor with the induction torque for starting. Significant magnetic saliency and reluctance torque at synchronous speed resulted from the difference in permeability between the rotor core and the permanent magnet. At asynchronous speed, the saliency and DC excitation of the permanent magnets will cause pulsating torque components. A LSPMSM may fail to synchronize when the field strength of the magnets is too strong, because of the excessive pulsating torque component from the DC excitation of the magnet. Since the stator and rotor of the LSPMSM are magnetically coupled, coupled circuit approach is used to develop a mathematical model of the motor. Based on rotary qd0 reference frame, mathematical model of LSPMSM has been developed. For completeness, the following shows a brief description of the mathematical modelling in the qd0 reference frame.

The equations of the stator and rotor voltages are defined as [11]:

$$\begin{bmatrix} v_{qs} \\ v_{ds} \\ v_{0s} \\ v_{qr} \\ v_{dr} \\ v_{0r} \end{bmatrix} = \begin{bmatrix} r_s & 0 & 0 & 0 & 0 & 0 \\ 0 & r_s & 0 & 0 & 0 & 0 \\ 0 & 0 & r_s & 0 & 0 & 0 \\ 0 & 0 & 0 & r_r & 0 & 0 \\ 0 & 0 & 0 & 0 & r_r & 0 \\ 0 & 0 & 0 & 0 & 0 & r_r \end{bmatrix} \begin{bmatrix} i_{qs} \\ i_{ds} \\ i_{0s} \\ i'_{qr} \\ i'_{dr} \\ i'_{0r} \end{bmatrix} + \frac{d}{dt} \begin{bmatrix} \lambda_{qs} \\ \lambda_{ds} \\ \lambda_{0s} \\ \lambda'_{qr} \\ \lambda'_{dr} \\ \lambda'_{0r} \end{bmatrix} + \begin{bmatrix} \omega \lambda_{ds} \\ -\omega \lambda_{qs} \\ 0 \\ 0 \\ 0 \\ 0 \end{bmatrix} \quad (1)$$

Where the primed quantities means the values referred to the stator side. Subscripts s, r referred to the stator and rotor, respectively. V_{qd0s} , V_{qd0r} are the q , d , 0 axis of the stator and rotor voltages, respectively. r_s , r_r are the stator and rotor resistances, respectively. i_{qd0s} , i_{qd0r} , λ_{qd0s} , λ_{qd0r} are the q , d , 0 axis of the stator and rotor currents and flux linkages, respectively. ω is the angular speed.

The end-ring resistance and magnetization currents are small. Hence both can be neglected. Therefore, the equivalent phase resistance of the motor can be expressed as:

$$r_r = \frac{(2NS)^2}{(Nb/3)} r_b \quad (2)$$

Where r_b is the rotor bar resistance. N_s is the number of stator winding turns. The q_{d0} axes of the stator and rotor flux components are defined as:

$$\begin{bmatrix} \lambda_{qs} \\ \lambda_{ds} \\ \lambda_{0s} \\ \lambda'_{qr} \\ \lambda'_{dr} \\ \lambda'_{0r} \end{bmatrix} = \begin{bmatrix} L_{ls} + L_{mq} & 0 & 0 & L_{mq} & 0 & 0 \\ 0 & L_{ls} + L_{md} & 0 & 0 & L_{md} & 0 \\ 0 & 0 & L_{ls} & 0 & 0 & 0 \\ L_m & 0 & 0 & L'_{lr} + L_{mq} & 0 & 0 \\ 0 & L_m & 0 & 0 & L'_{lr} + L_{md} & 0 \\ 0 & 0 & 0 & 0 & 0 & L'_{lr} \end{bmatrix} \begin{bmatrix} i_{qs} \\ i_{ds} \\ i_{0s} \\ i'_{qr} \\ i'_{dr} \\ i'_{0r} \end{bmatrix} + \begin{bmatrix} 0 \\ \lambda_m \\ 0 \\ 0 \\ \lambda_m \\ 0 \end{bmatrix} \quad (3)$$

Where L_{ls} is the stator leakage. L'_{lr} is the rotor leakage referred to the stator side and $L_{mq,d}$ is the q , d axis of the magnetizing inductances, respectively.

The torque equations of the LSPMSM are expressed as:

$$J \frac{d\omega_m}{dt} = T_e - T_L - B\omega_m \quad (4)$$

$$T_e = \frac{3p}{4} (i_{qs}\lambda_{ds} - i_{ds}\lambda_{qs})$$

Where J is the rotor moment of inertia. ω_m is the angular speed. P is the number of poles. T_e and T_L are the electromagnetic and load torques, respectively. B is the friction coefficient. Therefore, eqns. (1), (3) and (4) represent the mathematical model of LSPMSM.

Chapter 4

Thermal Modelling Background

Thermal modelling is about describing the thermal behavior of a system using mathematical means. It allows one to answer questions of how heat will be distributed depending on material properties and geometries, and how the system will react to changes in input [10].

To the benefit of those with a basic understanding of electronics, thermal systems are said to be analogous with electric circuits. That means that the equations and boundary conditions governing the behavior of one of the systems can be used to describe another by simply replacing the symbols of the variables, and the basic laws of electric circuits all apply for a corresponding thermal network. The relations between some important quantities are shown in Table 1.

Table 2: The relation between some electric and thermal quantities

Electrical Quantities		Thermal Quantities	
Potential	$V [V]$	Temperature	$\theta [^{\circ}K]$
Current	$I [A]$	Heat	$Q [W]$
Current density	$J [A/m^2]$	Heat flux	$q [W/m^2]$
Conductance	$G_{el} [S]$	Thermal conductance	$G_{th} [W/K]$
Conductivity	$\sigma_{el} [S/m]$	Thermal conductivity	$\lambda [W/mK]$
Resistance	$R_{el} [\Omega]$	Absolute Thermal resistance	$R_{th} [K/W]$
Resistivity	$\rho [\Omega/m]$	Thermal resistivity	$\rho_{th} [mK/W]$
Capacitance	$C_{el} [F]$	Thermal capacitance	$C_{th} [J/^{\circ}K]$

4.1 Heat Transfer Mechanisms

The second law of thermodynamics tells us that there is always net entropy increase in real processes. Entropy which is often described as the measure of disorder in a system, can also be used to describe the quality of the energy in a system. Low quality means a high level of disorder, and the highest possible entropy would be having the energy evenly distributed in space. Therefore, the second law of thermodynamics could also be explained by saying that an isolated system always strives for thermal equilibrium. Or, even more simply put, heat will flow from a hot place to a cooler place.

There are essentially three processes through which the transfer of heat can occur. Conduction is the transmission of energy between molecules in a medium. Although it is the only mechanism that takes place in solids, it is not exclusive to it, but takes place in fluids as well. The process is linear and can be described by

$$P = G (T_i - T_j) \quad (5)$$

Where P is the power flow, G is the thermal conductance, and T_i and T_j are the temperatures in two adjacent nodes.

In fluids and gases you also find the phenomena of convection. As the molecules in a non-solid medium are free to move around, the heat transfer ability of the medium is improved by the transportation of the molecules themselves, intermixing molecules of different energy levels and increasing the rate by which they come in contact with others. Just as for pure conduction, the mechanism is linear and can be described by (5). The third process is that of radiation, which describes the mechanism of a body emitting photons carrying energy. The amount of radiation a body emits

depends on the emissivity of the object, the surface area, but more strongly also the temperature. The net energy transfer can be described by:

$$P = G (T_i^4 - T_j^4) \quad (6)$$

In an electric machine, convection and radiation will contribute to the air gap and the frame-ambient thermal conductance. The effects of radiation tends to be rather small for electric machines, and will therefore be neglected. Furthermore, the process of predicting the motion of fluids can be very complicated and time consuming.

4.1.1 Thermal Resistance of Solids

Unlike properties such as mass or conductivity, thermal resistance of an object is calculated in respect to the direction of the heat flow.

The thermal conductance across a homogenous object can be calculated by:

$$G = \frac{\lambda A}{L} \quad (7)$$

where λ is the thermal conductivity, A the cross sectional area, and L the distance between the nodes. Accordingly, the thermal resistance is

$$R = \frac{1}{G} = \frac{L}{\lambda A} \quad (8)$$

Allowing the area of the conductor to vary over L results in the integral,

$$R = \int_0^L \frac{l}{\lambda A(l_{path})} dl_{path} \quad (9)$$

Which is the basic expression from which most resistance calculation methods are derived.

4.1.2 Thermal Resistance of Gases and Fluids

When making a thermal model representation of air, convection is a heat transfer process that needs to be considered. The modelling of air is a complex matter since fluid motion is dependent on so many factors, such as rotational speeds, surface structure, geometry dimensions, forced, flow, etc.

The thermal resistance between a solid surface and the ambient fluid can be written on the form:

$$R = \frac{1}{\alpha A} \quad (10)$$

Where A is the surface area subjected to convection, and α is the so called heat transfer coefficient [$W=m^2C$].

Finding α can be a challenging task requiring detailed knowledge of the machine. Achieving good values on some coefficient requires Computational Fluid Dynamics (CFD), a FEM based method demanding a lot of effort and expertise. Such detailed knowledge is however not always necessary for our “everyday” design requirements. Instead, it is often calculated by using formulas based on empirical studies. The behaviour of the movement of the air can be described by a few dimensionless numbers. The Nusselt number (Nu), the ratio of convective to conductive heat transfer normal to the boundary, is perhaps the one most closely related to the heat transfer coefficient. The relation with α can be written as

$$\alpha = \frac{\lambda_{Air} Nu}{2L} \quad (11)$$

$Nu = 2$ corresponds to a laminar flow, meaning that the molecules are only moving perpendicular to the normal of the plane. When that is the case,

(10) becomes the same as for any solid, which is seen if inserting (11) in (10). Nusselts number tend to be high for high rotor speeds and uneven surfaces, since those parameters increase turbulence. Several papers have made thorough investigations on how these parameters relate to each other for electric motors of different sorts, shapes and sizes for different points of operation.

4.2 Thermal Resistance Network Modelling

To find out the steady state behaviour of a thermal system, it can be represented with a network consisting of thermal resistances, heat flow and temperature sources. The conductance matrix of a system consisting of $n + 1$ nodes will look like:

$$G = \begin{bmatrix} \sum_{i=1}^n \frac{1}{R_{1,i}} & \frac{-1}{R_{1,2}} & \dots & \frac{-1}{R_{1,n}} \\ \frac{-1}{R_{2,1}} & \sum_{i=1}^n \frac{1}{R_{2,i}} & \dots & \frac{-1}{R_{2,n}} \\ \vdots & \vdots & \ddots & \vdots \\ \frac{-1}{R_{n,1}} & \frac{-1}{R_{n,2}} & \dots & \sum_{i=1}^n \frac{1}{R_{n,i}} \end{bmatrix} \quad (12)$$

Let a loss vector be defined to represent the power loss injected in each node,

$$P = \begin{bmatrix} P_1 \\ P_2 \\ \vdots \\ P_n \end{bmatrix} \quad (13)$$

and corresponding temperature vector,

$$\theta = \begin{bmatrix} \phi_1 \\ \phi_2 \\ \vdots \\ \phi_n \end{bmatrix} \quad (14)$$

representing the increase in temperature compared to the ambient temperature. Θ can be calculated by inverting the conductance matrix and multiplying it with the power vector, and thus getting an expression derived from ohm's law,

$$\Theta = G^{-1}P \quad (15)$$

Although setting up an accurate thermal network may require some work, the resulting model provides a means of getting quick solutions to changes in input parameters, since the mathematical complexity and number of necessary computations are low. The time taken to set up the model depends on the level of detail and accuracy needed for the engineering problem at hand.

4.3 Thermal Network Modelling Method

When a thermal resistance network is set up, there are many questions regarding for instance how to simplify the object in question, where to place the nodes, and how equivalent thermal resistances can be calculated for different shapes. This section presents principles and equations for developing a thermal network.

4.3.1 Nodalization

If a real object is to be represented with a circuit model consisting of a finite number of elements, some simplifications must inevitably be made. Nodalization is the concept of dividing an object into sub elements, where each element or connection point is represented by no more than one or possibly a few nodes. The notion of lumped parameter modelling means the simplified representation of the properties of the body in more manageable entities, such as average temperature, volume, and thermal mass.

An object may principally be divided into nodes in an arbitrary way, though there are naturally many things that should be taken into consideration. Some of these factors are where you need an accurate temperature prediction, what the expected temperature distribution looks like, and the ease of calculations of the resulting geometry. It can also be that a node needs to be placed somewhere where the point in itself is not of interest, but a connection is needed between other nodes or to increase the accuracy in the modelled flow path. Sticking to basic geometrical shapes makes the calculations of areas and volumes easy to calculate. In the case of the model being compared with actual measurements, it is advantageous to place nodes close to where the physical sensors are positioned.

The number of nodes can be chosen by the model designer based on the requirements on the resolution of the model. More nodes means getting more detailed information on different parts of a single section, or of a higher number of parts of an object. The price of having the extra accuracy of more nodes is an addition to the complexity of the network to analyze. Provided that the body is somewhat homogenous, making an interpolation between the temperatures of two adjacent nodal points can be a way of achieving acceptable estimation.

4.3.2 Lumped Parameter Thermal Element

When it is modelled by means of a lumped parameter network, an electrical machine is divided into several subdomains with a simpler geometry. In each subdomain, the temperature distribution can either be yielded by solving the network analytically or approximating it. Feasible shapes of the subdomain are for example rectangular or cylindrical solid. Using the analogy between thermal and electrical conduction, the thermal behaviour of the subdomain can be described with an electrical circuit. The network has thermal elements that consist of one central node to which a capacitor

and several resistors are connected. The potential of the central node is equivalent to the average temperature of the subdomain. Loss power is represented as a current source between the node and thermal ground. In order to calculate the transient behaviour, the temperature thermal capacities are added by connecting capacitors to the network's nodes.

4.4 Development of thermal network

Appropriate thermal resistance and thermal capacitance connect the nodes of the thermal network. The thermal resistance and capacitance are calculated from dimensional details of the machine [2], [3].

4.4.1 Calculation of Resistance between Frame and Ambient

When, heat transfer happens by convection (e.g. stator frame to ambient, stator core to frame and through air gap between stator and rotor), the resistance have to be determined by an empirical equation derived from the test data on the particular type of machine being analysed. The thermal resistance representing convective heat flow from the stator outer frame to ambient is given by the following equation:-

$$R_c = 1/(h.A_c) \quad (16)$$

The value of h is taken as:

$h \approx 5 - 25 \text{ W/m}^2 \text{ }^\circ\text{C}$ for free convection in air

$10\text{-}500 \text{ W/m}^2 \text{ }^\circ\text{C}$ for forced convection in air

4.4.2 Calculation of Frame Contact Resistance

When two separate surfaces come in contact, though we may assume that they are in perfect contact but the connecting surfaces touch only at discrete locations, due to surface roughness, interspaced with void spaces. The void spaces are usually filled with air. Thus there is no single plain of contact and the heat may flow in parallel paths through the contact point by conduction and through the void spaces by convection and perhaps by radiation. Thus a temperature drop occurs between the two materials at the interface. If T_A and T_B represent the temperatures of the two adjacent sides of the two material, total thermal resistance is defined by,

$$R_{tc} = (T_A - T_B)/Q \quad (17)$$

The thermal contact resistance is important to take into account the resistance offered to the heat flow at the interface between the outer diameter of the stator stamping and the frame. As expected, the metallic contact-resistance depends on the metals involved, the surface roughness, the contact pressure, the material occupying the void spaces and the temperature difference. The value of r_{tc} may be taken as 0.001

$m^2\text{°C/W}$ in the present case, where $R_{tc} = r_{tc}/A$

4.4.3 Calculation of Thermal Resistance of Air gap

At the air gap the stator and rotor acts as two concentric cylinders rotating relative to each other. The air-gap film coefficient, h is defined in terms of a dimension less Nusselt number, N_{nu} , the air gap length, l_g and the thermal conductivity of air K_{air} so that,

$$h = N_{nu} K_{air} / l_g \quad (18)$$

Taylor gives the value of the Nusselt number for the convective heat transfer between two smooth cylinders rotating with respect to one another. In an actual machine, however, there will be greater heat transfer across

the air gap than that is obtained for the smooth cylindrical surfaces, because of the additional fluid disturbances caused by the teeth and the slots. The Nusselt number (N_{nu}) for the small air-gap machines are obtained from the modified expressions as suggested by Taylor:

$$N_{nu} = 2.2 \text{ for } N_{Ta} \leq 41$$

$$N_{nu} = 0.23 N_{Ta}^{0.63} N_{Pr}^{0.27} \text{ for } 41 < N_{Ta} \leq 100 \quad (19)$$

The dimensionless Taylor number N_{Ta} and Prandtl number N_{Pr} are defined in terms of the air gap dimensions and fluid constants. The fluid constant values, which are temperature dependent, are taken at the expected full-load airgap temperature. The critical value 41 of the Taylor number refers to a change from laminar flow, which usually occurs in a small air-gap machine, to the turbulent flow in large air-gap machine. When the machine is stationary, the heat flow is assumed to be by conduction only, which represent a Nusselt number of 2.0.

4.4.4 Calculation of Thermal Resistance with End Shield

In the end cap region, single film coefficient is used to model the heat transfer to and from all the surfaces in contact with the circulating end-cap air. The value of end-cap film coefficients are found from an approximate linearized equation for cooling air velocities v as,

$$h = 15.5(0.29v + 1) \text{ W/m}^2\text{K} \quad (20)$$

The constant term in the expression represents the heat transfer by natural convection alone. The cooling air velocity v may be estimated from,

$$v = r_m \omega_r \eta \quad (21)$$

where r_m is the log-mean radius of end-ring fins, ω_r is the rotor angular velocity and η is the fan efficiency. Because of the lack of available

information on the radial air velocity, an arbitrary value of 50% was assumed for the fan efficiency.

4.4.5 Plane Wall with Specified Boundary Temperatures

An elementary conduction problem is that of a plane wall of finite thickness but infinite in extent in all other directions, with each face maintaining a specific temperature and having a constant conductivity. The rate of heat flow through the wall may be readily deduced from the Fourier's law and is given by,

$$Q = KA_s(T_1 - T_2)/\delta x$$

$$or, (T_1 - T_2) = Q \delta x / (K A_s) = Q R_{Th} \quad (22)$$

4.4.6 Cylinders with Specified Temperature

The inner surface of radius, r_1 and outer surface of radius, r_2 are maintained at uniform temperature T_1 °C and T_2 °C respectively. Under the steady state condition, the heat flow across any cylindrical surface having a radius r , is constant and is given by the Fourier's law as stated bellow,

$$Q = -KA_r dT/dr \quad (23)$$

$$So, R = \ln(r_2/r_1)/(2\pi KL) \quad (24)$$

where, $A_r = 2\pi rL$, L being the length of the cylinder. Based on the above formulation the thermal resistance between the consecutive nodes can be calculated.

The thermal resistance of all the other parts of the machines, i.e., stator and rotor core, stator and rotor teeth, stator and rotor slot is determined from relationship depicted in eq. 22 and eq. 24, whichever is applicable.

4.4.7 Calculation of Thermal Capacitances

In order to simulate the transient behavior of the machine, thermal capacitances have been defined, their number being equal with that of the considered nodes. Each capacitor in the thermal network represents the heat capacity of the respective part of the machine.

Thermal capacity $C_{th}(J/^{\circ}C)$ depends on the volume of the segment $V_n(m^3)$, the density of the material $\rho_v(kg/m^3)$ and specific heat $C_{ths}(J/kg^{\circ}C)$ of the material as follows:

$$C_{th} = V_n \cdot \rho_v \cdot C_{ths} \quad (25)$$

Chapter 5

A Lumped Parameter Thermal Network Model (LPTN)

A lumped parameter thermal network (LPTN) is a simplified model of the heat flow and temperature distribution inside an electric motor. It divides the motor into a number of discrete nodes, each of which is assigned a single temperature. The heat transfer between the nodes is modeled by thermal resistances, and the heat generation in each node is modeled by a heat source. The thermal capacitance of each node represents the ability of the node to store heat.

The LPTN can be used to simulate the transient (time-varying) behavior of the motor's temperature at each node, as well as the steady-state behavior.

In this work, a LPTN has been developed for obtaining the heat flow within the LSPMSM, and its schematic is shown in Figure 5 (a). A preliminary selection of the resistances and capacitances was determined according to the geometry of the motor and from the physical properties of the material used.

Fig.5 (a) shows the proposed thermal network. The different nodes considered for the model are shown on the drawing. Given nodes have been considered, namely, ambient, frame, stator core , stator slot, stator teeth, air gap, rotor slot, rotor teeth, rotor core upper, PM, rotor core lower and shaft & on both Driving End & Non Driving End.

5.1 LPTN model and simulation

Table - 3

Motor Name plate data.	
Kilowatt	11 KW
Ampere	17 A
Voltage	415 V
Pole	4
Frame Size	160M
Frequency	50 Hz
Efficiency	95 %
Ambient	35°C
Power Factor	0.85

A Lumped Parameter Thermal Network (LPTN) model of a motor has been simulated in Matlab. The model incorporates the thermal resistances, capacitances, and losses of the machine. The calculations were performed using the dimensional and nameplate data of the motor.

To accurately represent the heat transfer within the motor, both radial and axial thermal resistances were taken into account for the ambient, frame, stator core, stator teeth, air gap between the stator and rotor, rotor slot, rotor teeth, rotor core upper section, permanent magnet (PM), rotor core lower section and the shaft.

Additionally, radial thermal resistance was considered for the end cover, bearing and shaft located at both driving and non-driving ends of the machine. Although the contributions of these components to the overall heat transfer mechanism were minimal and could be considered negligible.

Nodes within the model were interconnected with losses and thermal capacitance. Below is a list of the nodes that were considered in the analysis:

- Frame
- Stator Core
- Stator Slot
- Stator Teeth
- Air Gap
- Rotor Teeth
- Rotor Slot
- Rotor Core Upper Section
- Permanent Magnet
- Rotor Core Lower Section
- Shaft

Each of these nodes was associated with resistances, denoted by R1 to R46, accounting for both axial and radial directions.

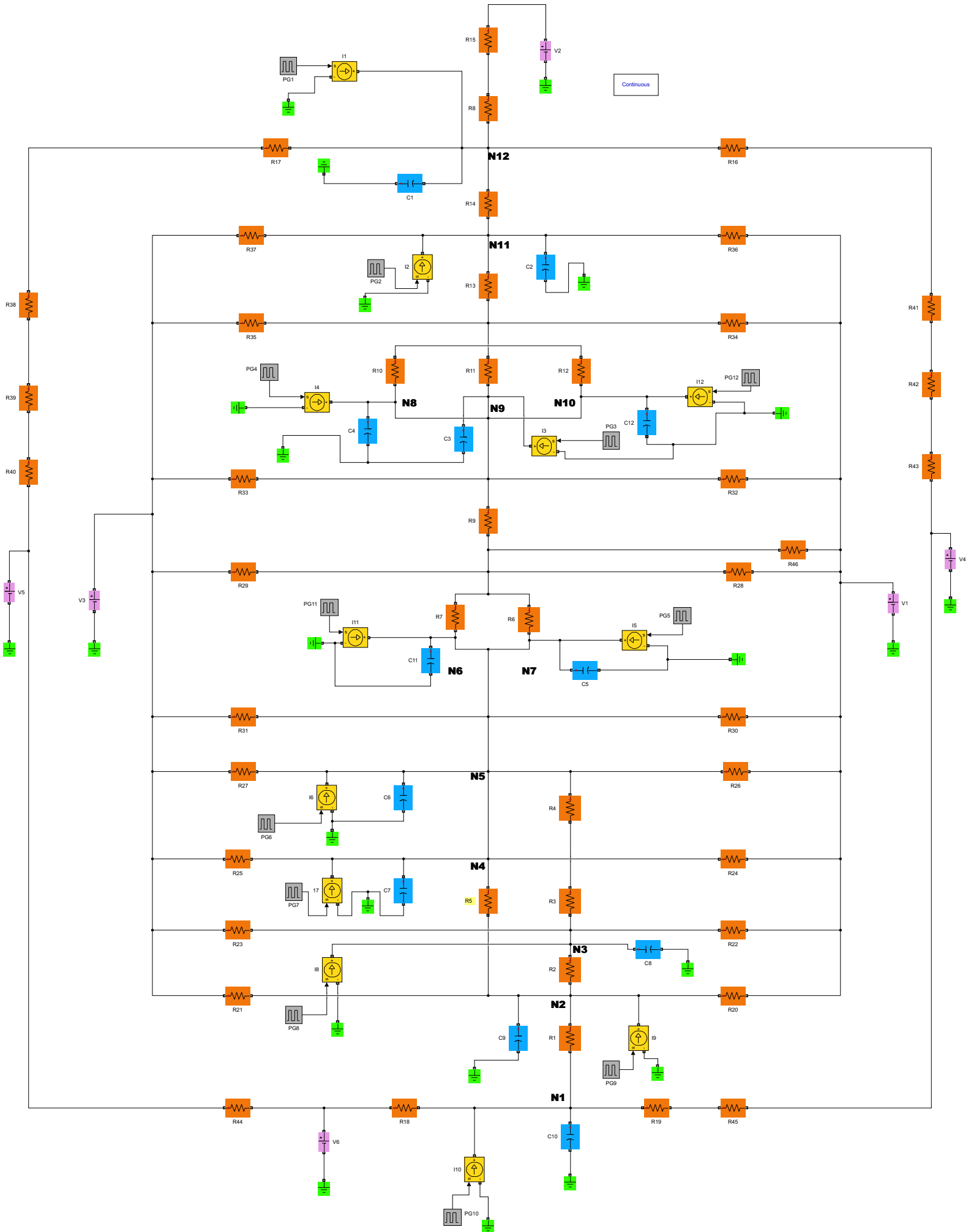


Fig – 5(a) Schematic diagram of LPTN model

5.2 Results and observation.

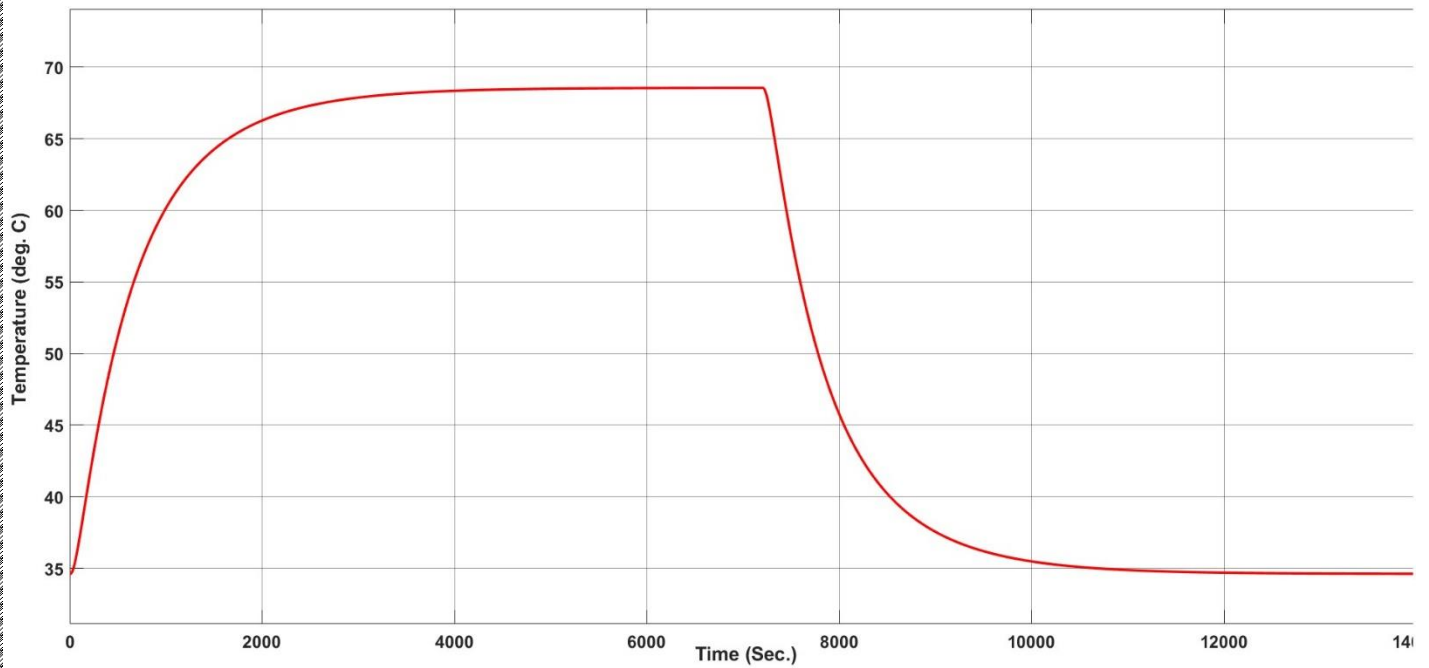


Fig – 5(b) Simulated temperature rise in Frame of Motor

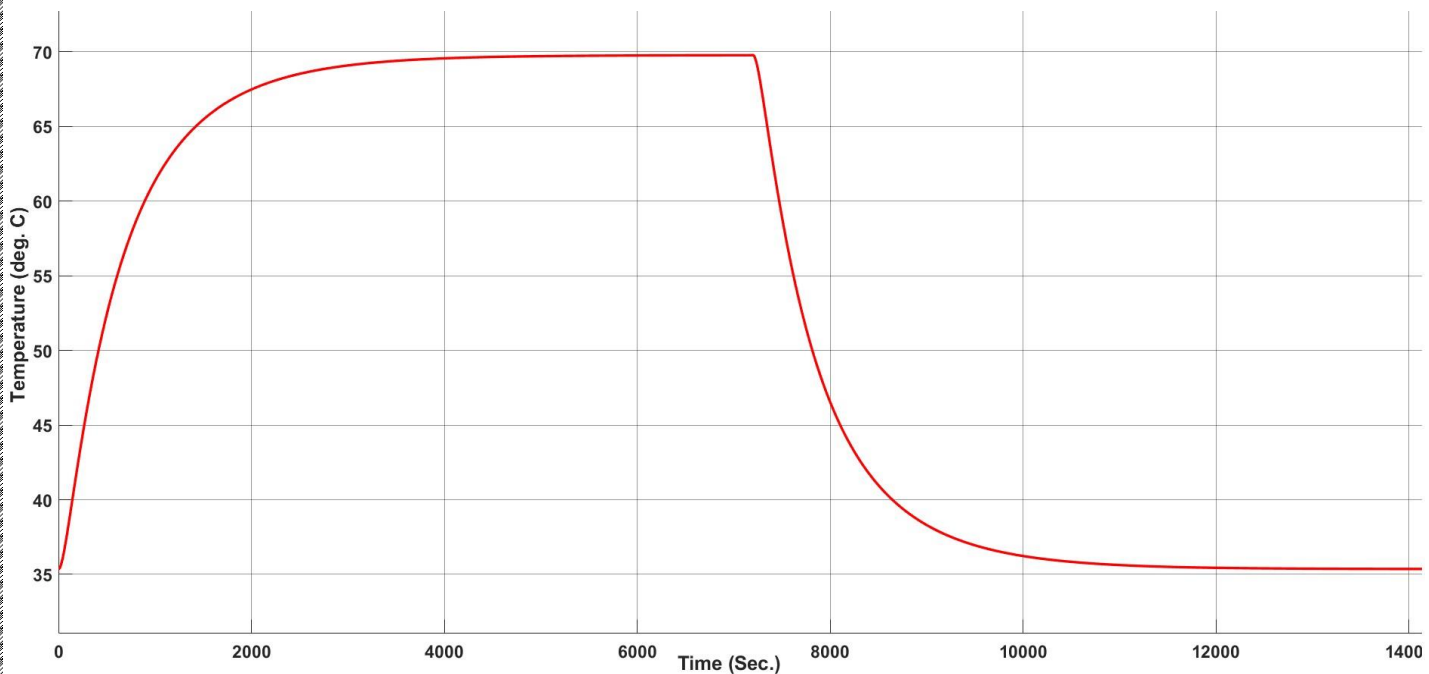


Fig – 5(c) Simulated temperature rise in Stator core of Motor

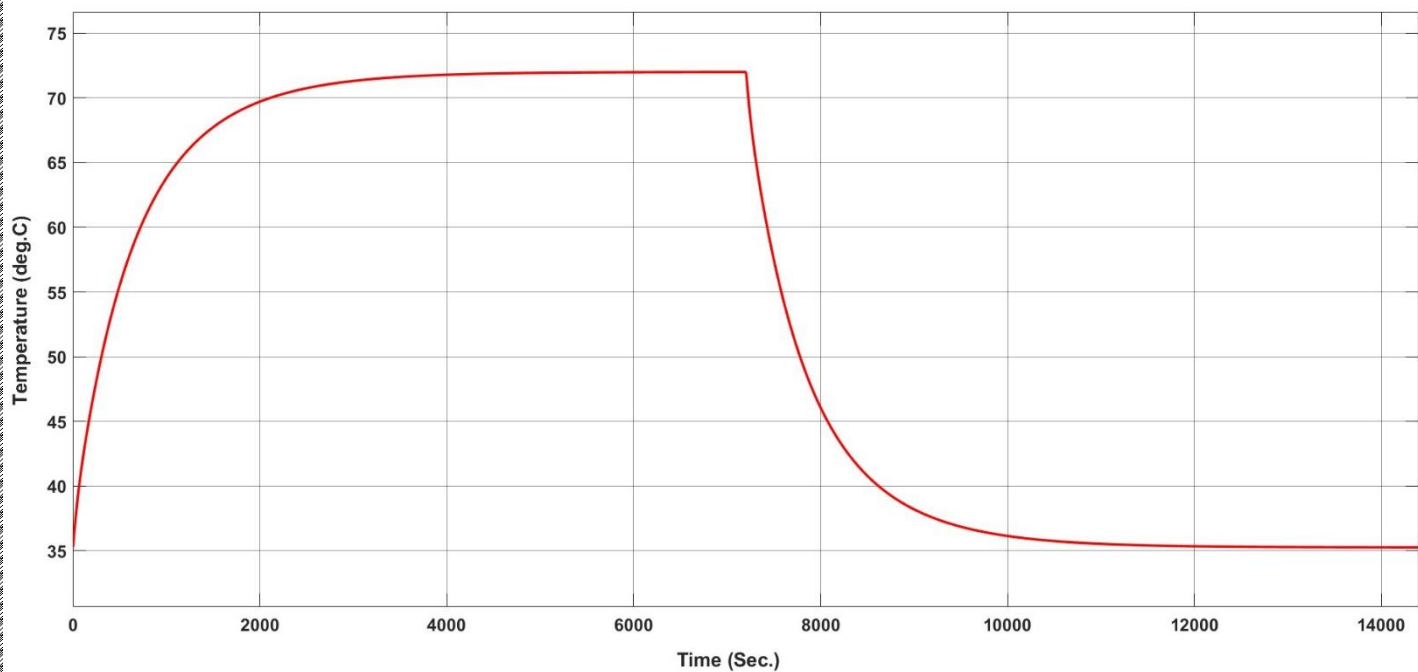


Fig – 5 (d) Simulated temperature rise in Stator conductor of Motor.

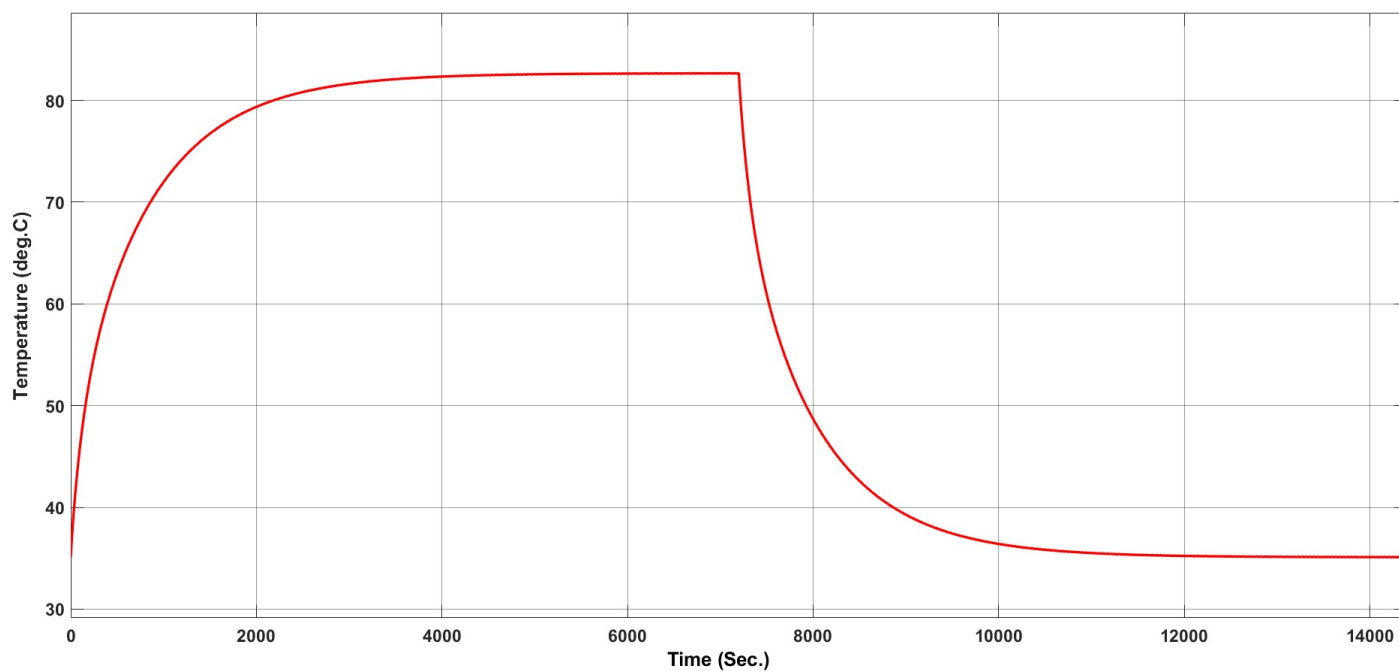


Fig – 5 (e) Simulated temperature rise in Rotor Upper core of Motor.

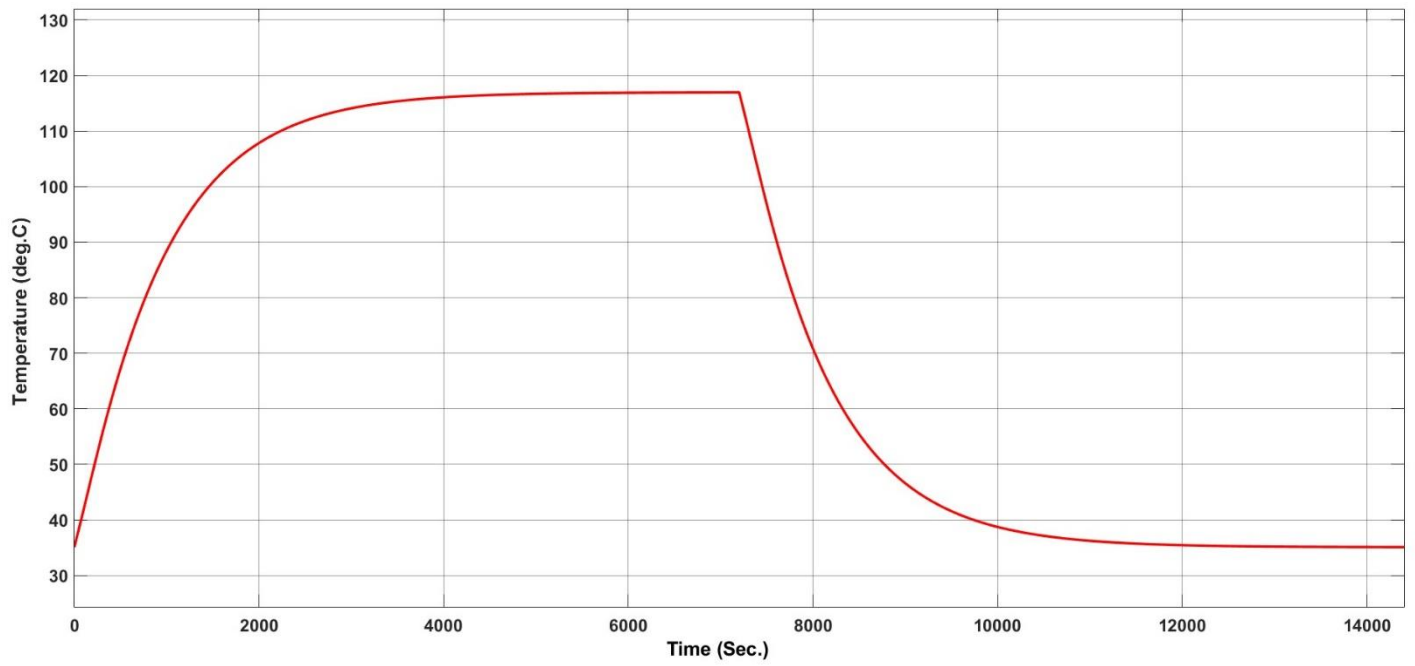


Fig – 5 (f) Simulated temperature rise in PM of Motor

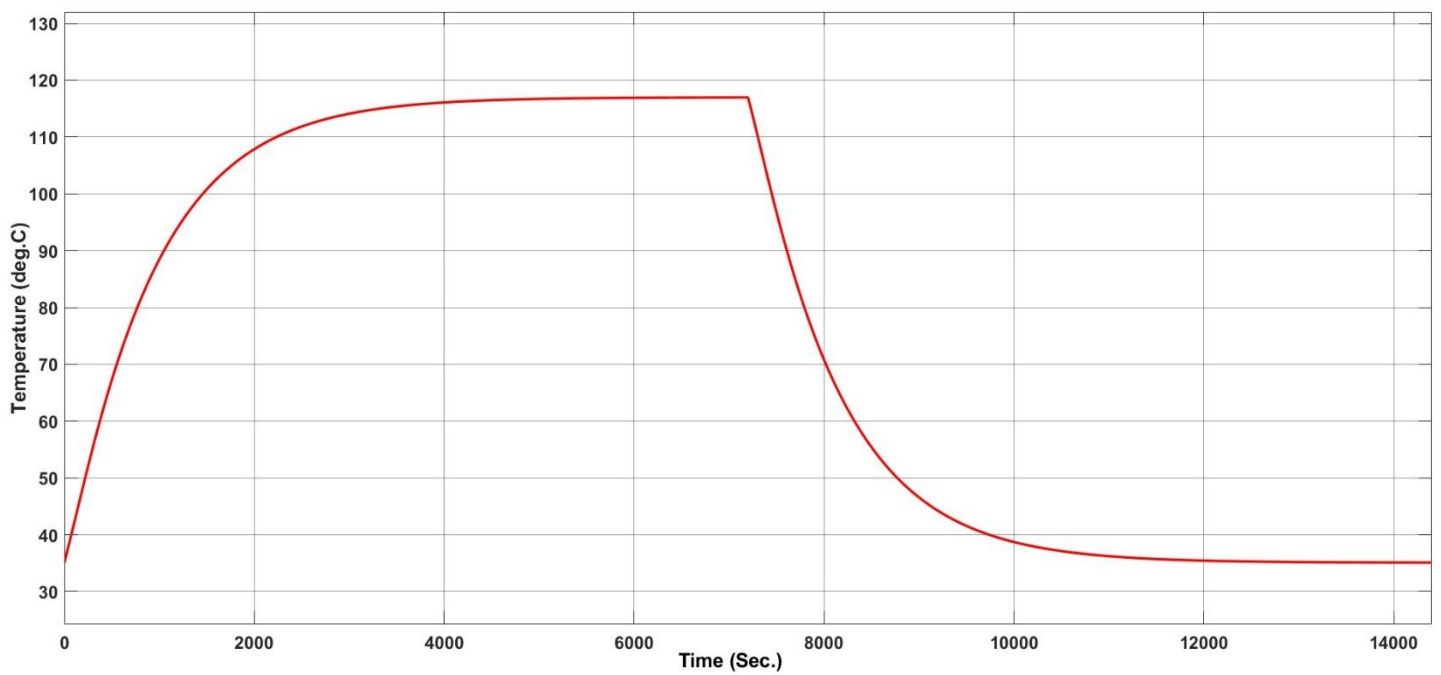


Fig – 5 (g) Simulated temperature rise in Lower core of Motor

The simulation results have revealed valuable insights into the thermal behavior of the system. Specifically, the temperature rise curve, provide critical information about the system's thermal performance. Here's an elaboration on the observations and their implications:

Temperature Variation from Ambient to Steady State: The simulation results have generated a temperature rise curve that shows how the temperature within the system changes over time. This data is essential for understanding how the system responds to different operating conditions.

Gradual Temperature Increase from Frame to Rotor Lower Core: One noteworthy observation is that as we move from the "frame" node to the "rotor lower core" node along the system, the temperature gradually increases. This indicates that heat is being generated and transferred through the various components, causing a temperature gradient within the motor. The gradual temperature increase implies that certain components are dissipating more heat than others or that there might be variations in thermal conductivity across different parts of the motor.

Chapter 6

Conclusions

The development of an LPTN for LSPMSM with the aim of determining the temperature rise in various machine parts was the focus of this paper. In pursuit of this objective, the LPTN network method was expounded upon, encompassing the calculation of thermal resistances, capacitances, and power losses.

The LPTN model is considered a suitable compromise between accuracy and computational speed for the thermal analysis of line start permanent magnet synchronous motors (LSPMSM). The capability to predict temperature distribution inside an LSPMSM accurately is a distinguishing feature of the LPTN model. Furthermore, it offers a simpler and faster alternative to the use of FEA models. This renders it suitable for application during the early design phases of PMSMs when a rapid and precise estimation of temperature rise is imperative.

Potential hotspots within the motor are highlighted by the gradual temperature increase. These are areas where concerns related to heat generation or inadequate heat dissipation may arise. During the design phase, emphasis on the optimization of the thermal properties of these critical components to avert overheating is necessitated.

Taking actual temperature data from the thermal run of the considered motor will enable to validate this model in the future.

The observations will shed light on the formulation of effective thermal management strategies. These strategies may encompass the utilization of heat sinks, cooling mechanisms, or enhanced materials in regions where temperature rise is more pronounced.

Ensuring that the temperature rise remains within acceptable limits is deemed crucial for the motor's efficiency and long-term reliability. Design adjustments can be implemented to sustain safe operating temperatures and prolong the motor's operational life.

An understanding of thermal behaviour can also lead to the optimization of performance by minimizing temperature gradients and effectively managing heat.

6.1 Future scope of work

The future scope of work in thermal modelling of electric motors is wide and promising. A critical aspect of thermal modelling is accurate material properties. Future research can focus on better characterization of materials used in PMSMs, especially advanced materials like high-temperature magnets and insulating materials. This can lead to more precise modelling results. Furthermore, developing optimization algorithms that take thermal constraints into account during motor design can lead to more energy-efficient PMSMs. This includes optimizing the geometry, winding patterns, and cooling systems to maximize performance while ensuring safe temperature levels.

And with the growing popularity of electric vehicles (EVs), research into thermal modelling of PMSMs in EV propulsion systems will continue to be relevant. This includes optimizing motor design for higher power density and thermal management strategies for extended battery and motor life.

References

- [1] D. Liang et al., "A Hybrid Lumped-Parameter and Two-Dimensional Analytical Thermal Model for Electrical Machines," in *IEEE Transactions on Industry Applications*, vol. 57, no. 1, pp. 246-258, Jan.-Feb. 2021, doi: 10.1109/TIA.2020.3029997.
- [2] S. K. Chowdhury and P. K. Baski, "A simple lumped parameter thermal model for electrical machine of TEFC design," 2010 Joint International Conference on Power Electronics, Drives and Energy Systems & 2010 Power India, New Delhi, India, 2010, pp. 1-7, doi: 10.1109/PEDES.2010.5712385.
- [3] A. Kačenka, A. -C. Pop, I. Vintiloiu and D. Fodorean, "Lumped Parameter Thermal Modeling of Permanent Magnet Synchronous Motor," 2019 Electric Vehicles International Conference (EV), Bucharest, Romania, 2019, pp. 1-6, doi: 10.1109/EV.2019.8892937.
- [4] G. Sooriyakumar, R. Perryman and S. J. Dodds, "Analytical thermal modelling for permanent magnet synchronous motors," 2007 42nd International Universities Power Engineering Conference, Brighton, UK, 2007, pp. 192-196, doi: 10.1109/UPEC.2007.4468945.
- [5] D. Liang et al., "A Hybrid Lumped-Parameter and Two-Dimensional Analytical Thermal Model for Electrical Machines," in *IEEE Transactions on Industry Applications*, vol. 57, no. 1, pp. 246-258, Jan.-Feb. 2021, doi: 10.1109/TIA.2020.3029997.
- [6] C. Liu, J. Zou, Y. Xu and G. Yu, "An Efficient and High Fidelity Thermal Computation Model of Permanent Magnet Synchronous Motor," 2020 IEEE International Conference on Applied Superconductivity and

Electromagnetic Devices (ASEMD), Tianjin, China, 2020, pp. 1-2, doi: 10.1109/ASEMD49065.2020.9276357.

[7] J. -Y. Ryu, S. -W. Hwang, J. -W. Chin, Y. -S. Hwang, S. W. Yoon and M. -S. Lim, "Mathematical Modeling of Fast and Accurate Coupled Electromagnetic-Thermal Analysis," in IEEE Transactions on Industry Applications, vol. 57, no. 5, pp. 4636-4645, Sept.-Oct. 2021, doi: 10.1109/TIA.2021.3086823.

[8] M. F. Palangar, W. L. Soong and A. Mahmoudi, "Outer and Inner Rotor Line-Start Permanent-Magnet Synchronous Motors: An Electromagnetic and Thermal Comparison Study," 2021 IEEE Energy Conversion Congress and Exposition (ECCE), Vancouver, BC, Canada, 2021, pp. 4226-4233, doi: 10.1109/ECCE47101.2021.9595574.

[9] D. S. B. Fonseca, Carlos M. C. Santos & Antonio J. Marques Cardoso. "Modelling of a Line-Start Permanent Magnet Synchronous Motor, Using Empirical Parameters". ICEUBI2017 - INTERNATIONAL CONGRESS ON ENGINEERING 2017 – 5-7 Dec 2017 – University of Beira Interior – Covilhã, Portugal.

[10] BJÖRN ANDERSSON “Lumped Parameter Thermal Modelling of Electric Machines. Analysis of an Interior Permanent Magnet Synchronous Machine for Vehicle Applications”. PhD thesis. Chalmers University of Technology, Göteborg, Sweden, 2013.

[11] Baradie, Khalid & Hamouz, Zakariya. (2018). Modelling and Simulation of Line Start Permanent Magnet Synchronous Motors with Broken Bars. Journal of Electrical & Electronic Systems. 07. 10.4172/2332-0796.1000259.

[12] M. J. Bala, N. K. Deb and S. K. Chowdhury, "Improvement of the performances of line start permanent magnet synchronous motor with flux barrier in the rotor," 2017 IEEE Calcutta Conference (CALCON), Kolkata, India, 2017, pp. 357-361, doi: 10.1109/CALCON.2017.8280755.

[13] M. J. Bala, C. Jana, S. K. Chowdhury and N. K. Deb, "Performance analysis of different rotor configuration of LSPMSM for Electric Vehicles," 2022 IEEE Calcutta Conference (CALCON), Kolkata, India, 2022, pp. 223-227, doi: 10.1109/CALCON56258.2022.10060046.

[14] M. Baranski, W. Szelag and C. Jedryczka, "Influence of temperature on partial demagnetization of the permanent magnets during starting process of line start permanent magnet synchronous motor," 2017 International Symposium on Electrical Machines (SME), Naleczow, Poland, 2017, pp. 1-6, doi: 10.1109/ISEM.2017.7993535.

[15] Aziz, Rebaz & Atkinson, G. & Salimin, Suriana. (2017). Thermal Modelling for Permanent Magnet Synchronous Machine (PMSM). International Journal of Power Electronics and Drive Systems (IJPEDS). 8. 1903. 10.11591/ijpeds.v8.i4.pp1903-1912.

[16] Jacek F. Gieras, Mitchell Wing; "Permanent Magnet Motor Technology Design and Application; Second Edition; Marcel Dekker, Inc.; 2002.

[17] D. Staton, S. J. Pickering, and D. Lampard, "Recent advancement in the thermal design of electric motors," Proc. SMMA—Fall Tech. Conf., Oct. 3–5, 2001.

[18] A. Boglietti, A. Cavagnino, D. Staton, M. Shanel, M. Mueller, and C. Mejuto, "Evolution and modern approaches for thermal analysis of

electrical machines,” IEEE Trans. Ind. Electron., vol. 56, no. 3, pp. 871–882, 2009.

[19] P.H. Mellor, D. Roberts, and D.R Turner, “Lumped parameter thermal model for electrical machines of TEFC design,” IEE Proc.-B, vol. 138, no. 5, pp. 205-218, 1991.

[20] G. Demetriades, H. D. L. Parra, E. Andersson, and H. Olsson, “A real-time thermal model of a permanent-magnet synchronous motor,” IEEE Trans. Power Electron., vol. 25, no. 2, pp. 463–474, 2010.

[21] A. Boglietti and A. Cavagnino, “Determination of critical parameters in electrical machine thermal models,” IEEE Trans. Ind. Appl., vol. 44, no. 4, pp. 1150–1159, 2008.

[22] D. A. Staton and A. Cavagnino, “Convection heat transfer and flow calculations suitable for electric machines thermal models,” IEEE Trans. Ind. Electron., vol. 55, no. 10, pp. 3509–3516, 2008.

[23] R. T. Ugale, B. N. Chaudhari “A new rotor structure for line starts permanent magnet synchronous motor” IEEE, 2013.

[24] R. T. Ugale, B. N. Chaudhari, Srinivas Baka “Inset-Consequent and Inset Rotors for Line Start Permanent Magnet Synchronous Motor”, p. 333-338, 2012 IEEE.

[25] S. Peter, H A. Valeria, R. Pavol, K. Lukas and O. Matus” Effect of Permanent magnet Rotor Design on PMSM properties” Transaction on Electrical Engineering, Vol. 1 (2012), No. 3.